

Time evolution of stimulated Brillouin scattering during transverse laser pumping of carbon disulfide filling a capillary

A. I. Erokhin, V. S. Starunov, and A. K. Shmelev

P. N. Lebedev Physics Institute, Russian Academy of Sciences, 117924 Moscow, Russia

(Submitted 16 November 1994)

Pis'ma Zh. Eksp. Teor. Fiz. **60**, No. 12, 823–828 (25 December 1994)

The time evolution of the intensity of stimulated Brillouin scattering has been studied experimentally during transverse laser pumping of carbon disulfide filling a glass capillary. The scattered light was detected from the ends of the capillary. Large-scale temporal oscillations of the scattering intensity are observed, with time intervals on the order of and greater than the time taken by the light to traverse the length of the capillary twice. A small-scale temporal modulation is also observed. The modulation periods are equal to the period of the hypersonic wave in the stimulated Brillouin scattering and its subharmonics. © 1994 American Institute of Physics.

Stimulated Brillouin scattering (or “stimulated Mandel’shtam–Brillouin scattering”) has been the subject of a large number of studies, but there have been only a few experimental studies^{1,2} of the time evolution of the spectrum at a time resolution on the order of or better than the period of the hypersonic wave. These studies and several experiments in glass optical fibers (e.g., Refs. 3 and 4) have shown that there is a promising outlook for research on various dynamic effects, bifurcations, and the road to dynamic chaos through measurements of time-resolved spectral characteristics of stimulated scattering of light—of stimulated Brillouin scattering (SBS), in particular. In previous studies, the stimulated-scattering light propagated collinearly with the pump light.

In this letter we are reporting an effort to experimentally study the sequence of the onset and time evolution of various spectral components of stimulated scattering in a thin glass capillary filled with liquid carbon disulfide during transverse laser pumping.

1. The stimulated scattering was excited by the second harmonic from a single-mode neodymium laser (530 nm) with a duration $t_p \approx 15$ ns (at half-maximum) and a maximum energy of 200 mJ. This light was expanded to dimensions ~ 6 cm and then focused by a cylindrical lens into the capillary holding the CS₂. The capillary had an inside diameter of 170 μm and a length $L = 18$ cm (the time required for a double traversal of the capillary by light was $2T_0 = 2Ln/c = 2$ ns; the corresponding time for traveling between the exit windows was $2T_1 \approx 2.3$ ns). Small windows in the capillary were skewed with respect to the axis of the capillary. The stimulated scattering from the end of the capillary was resolved spectrally by a Fabry–Perot interferometer (with a dispersion region 1–2.5 cm^{-1}) and sent to the slit of an Agat image-converter camera. The time evolution of the spectrum was determined. Measures were taken to check for the onset of stimulated Raman scattering. We also carried out some experiments in which the stimulated scattering was detected from the two ends of the capillary simultaneously, with the help of

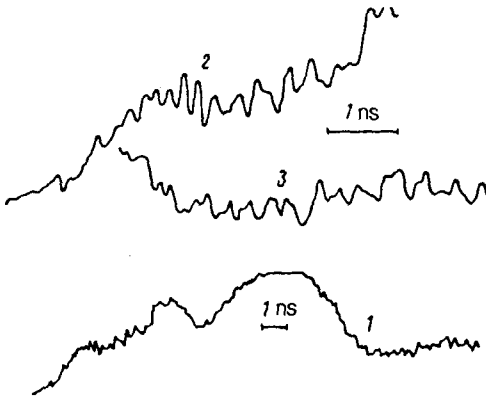


FIG. 1. Photomicrograph of a time sweep of the SBS-90 (1) and fragments at a scale five times larger of the beginning (2) and end (3) of this sweep.

FK-26 photodetectors and an S7-19 oscilloscope with a bandwidth of 1 GHz.

2. A stimulated Brillouin scattering was excited at fairly low threshold intensities. In terms of the spectral shift from the pump line ($\Delta\nu \sim 0.18 \text{ cm}^{-1}$), it corresponded to Stokes scattering at an angle $\vartheta = 90^\circ$ (we will refer to this case below as SBS-90). When the pump energy was raised, a stimulated-Brillouin line which corresponded (in terms of spectral shift from the SBS-90 line: 0.26 cm^{-1}) to scattering at an angle $\vartheta = 180^\circ$ from the SBS-90 light appeared (below, we will refer to this second line as SBS-180). At even higher pump power levels, the following Stokes lines and also anti-Stokes lines of SBS-180 appeared. A stimulated Raman scattering also arose; the latter scattering had a strong influence on the time evolution of the stimulated Brillouin scattering. In this letter we are reporting the results on the temporal characteristics of the SBS-90 and of the SBS-180 which arose from it under conditions such that stimulated Raman scattering was not excited.

3. Just above the detection threshold, the SBS-90 oscilloscope traces are smooth and bell-shaped. The pump pulse does not have any apparent temporal or spatial asymmetry, but the SBS-90 emission from the two ends of the capillary is frequently unequal: One can observe SBS-90 from one end but not the other. This situation is evidence of a substantial difference in the intensities here. The temporal oscillations in the SBS-90 emission from one end of the capillary which arise as the pump power is increased near the intensity maximum are not seen in the emission from the other end. The distance between the peaks of these oscillations is in the interval $\sim 1.5\text{--}4 \text{ ns}$; it usually increases as the SBS process develops.

4. The time evolution of these large-scale oscillations was studied by means of a time sweep of the spectrum on an image-converter camera. As an example, curve 1 in Fig. 1 shows a photomicrograph of a time sweep of the SBS-90 under conditions such that there is also a weak SBS-180 component in the second half of the pulse. The onset of the first SBS-180 component does not have any noticeable effect on the time evolution of the SBS-90. The time intervals between the oscillation peaks usually increase as the SBS process develops, from ~ 2 to $\sim 6 \text{ ns}$. In the case of Fig. 1, the distance between the oscillations peaks increases in the sequence 3.1–3.4, 4.1–4.7, 5.8–6.2 ns. There is one more peak between the first and second. In another typical case, the sequence of pulses is

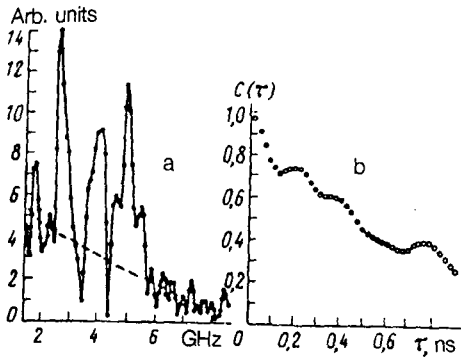


FIG. 2. a—Fourier spectrum; b—correlation function $C(\tau)$ of the initial stage of the development of the SBS-90.

1.8–2, 2.9–3.1, 6 ns. Less typical is situation in which the intervals between pulses goes through a maximum: 3.5–4, 4.5–5.2, 3.5–3.8, 3.5–4 ns. Sometimes, groups of much weaker pulses, with intervals of 0.45–0.7 ns, are observed before the first oscillation and after the last one.

On the time sweep, we frequently detect two interferogram orders of different intensities, in which the relative positions and time intervals of the time oscillation peaks are not always the same.

5. The first SBS-180 component, which arises from the SBS-90, is detected slightly before or after the intense SBS-90 oscillation. The temporal structure of the SBS-180 is qualitatively similar, in general features, to the SBS-90 structure, although the total duration and the number of oscillations are smaller, and their temporal maxima and minima often do not coincide with those of the SBS-90.

6. Against the background of the large-scale oscillations described above, we observe fluctuations and oscillations (a periodic modulation) of the intensity which are of small scale in time. These features are particularly clear in the initial and final stages of the development of the process and at the beginning and end of the large-scale oscillations, with a depth up to 50%. As an example, Fig. 1 shows fragments of the initial (2) and final (3) stages of the time sweep of the SBS-90, enlarged by a factor of 5. Visually, at the beginning of the pulse on the photograph of the time sweep, we can clearly see a periodic structure with a period (found from measurements on a comparator) $T_1 = 0.2\text{--}0.22$ ns ($f_1 = 1/T_1 \approx 5.0\text{--}4.6$ GHz). This value is close to the period of the hypersonic wave in the SBS-90 ($T_1 \sim 0.19$ ns, $f \sim 5.4$ GHz). As the process develops, we can clearly see structure with an approximately doubled period, 0.35–0.41 ns (2.9–2.4 GHz). This subharmonic structure is seen even more clearly at the end of the pulse. On some of the time sweeps it is possible to also detect structures with periods $T_2 \sim 0.1\text{--}0.15$ ns and 0.3 ns, close to the period of the hypersonic wave in SBS-180 ($f_2 \sim 7.7$ GHz, $T_2 \sim 0.13$ ns) and its second harmonic.

7. A Fourier analysis of the initial stage of the time evolution of the SBS-90 was carried out on a computer to clarify the observed picture. The integral $I(f_i) = \int I(t) \exp(2i\pi f_i t) dt$ was calculated for a set of frequencies from $f_1 = 1.42$ GHz to $f = 8.5$ GHz at steps of $f = 7.1 \times 10^{-2}$ GHz. The integration step was 2.2×10^{-2} ns, and the integration interval 8.2 ns. In this manner we constructed a spectrum $I(f_i)$ (Fig. 2a)

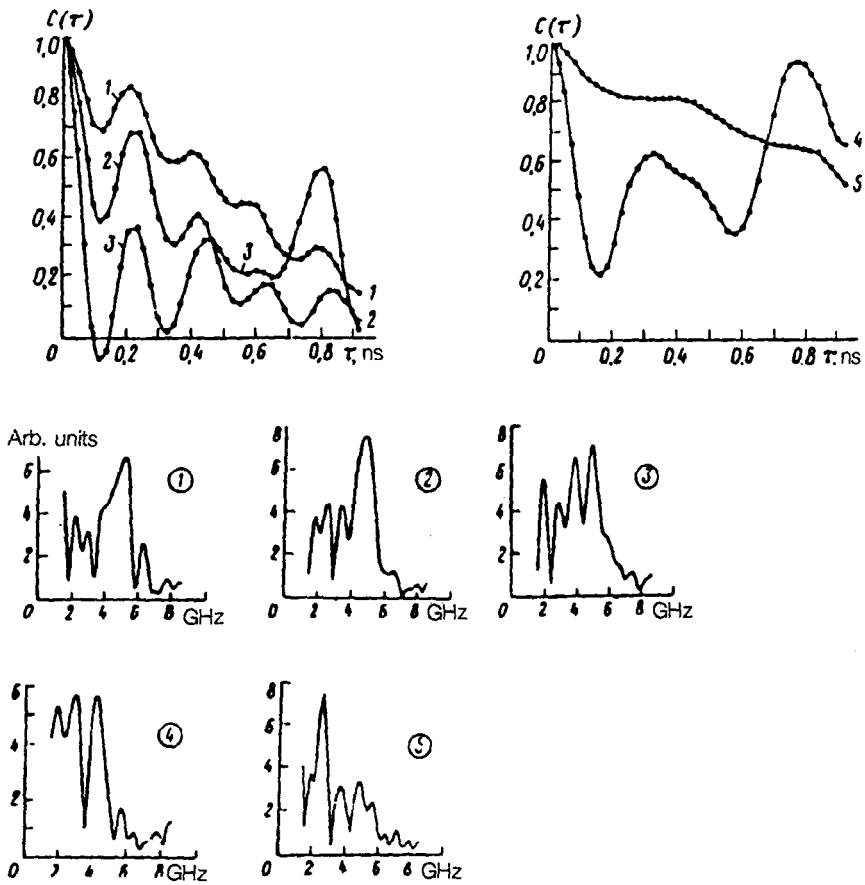


FIG. 3. Fourier spectra (lower row) and $C(\tau)$ (upper row) for intervals smaller than those in Fig. 2 (see the discussion in the text proper).

for the time interval spanning the first two large-scale oscillations in Fig. 1 and half of the third oscillation. Corresponding calculations were carried out for shorter integration intervals by breaking up the preceding interval into eight partially overlapping regions. Figure 3 shows the first through fifth of these spectra (the lower row). Correlation functions $C(\tau) = \int I(t)I(t + \tau)dt$ were calculated for the same intervals. Figure 2b shows functions $C(\tau)$ for the entire analyzed region (8.2 ns); Fig. 3 shows them for shorter time interval (at the top). In this analysis (Figs. 2 and 3), the initial time dependence of the intensity (the blackening) was first smoothed in order to eliminate large-scale oscillations, through a numerical simulation of an RC differentiating circuit. A calculation of the Fourier spectra and $C(\tau)$ of the same time sweep (Fig. 1) with other partition time intervals, with frequency and integration steps smaller by a factor of 4, and with the large-scale oscillations eliminated by reading the signal from an envelope drawn through the minima of the small-scale fluctuations, leads to qualitatively the same result and does not change the positions of the maxima in the Fourier spectrum.

Several groups of frequencies can be distinguished in the spectra (Figs. 2 and 3). The groups of frequencies in the regions 4.6–5.9 and 2.3–3 GHz in $C(\tau)$ in Fig. 2b can be associated with maxima in the regions 0.17–0.22 and 0.32–0.38 ns, in accordance with direct measurements on the film (Sec. VI). These features can be associated with a modulation of the scattered hypersonic-wave emission in the case of the SBS-90 ($f_1 \approx 5.4$ GHz) and its subharmonic $f = 1/2f_1$. Within the indicated limits (4.6–5.9 GHz), they are also seen in the spectra and $C(\tau)$ for smaller integration intervals (Fig. 3).

In the spectra in Figs. 2 and 3 we can see some less intense groups of frequencies in the region $f_2 \sim 7$ –8.2 GHz and also in the interval 3.7–4.2 GHz (curves 3–5 in Fig. 3), which can be associated with subharmonics of the frequencies f_2 . They can be interpreted as the result of a modulation of the scattered hypersonic-wave light ($f_2 = 7.7$ GHz) and its subharmonic of frequency $(1/2)f_2$ in the SBS-180.

In the spectra described here we usually observe not isolated frequencies corresponding to the SBS-90 (f_1) and the SBS-180 (f_2) or their subharmonics but groups of frequencies (two to five frequencies) in their vicinity, separated by intervals of 0.1–0.5 GHz, which change in position and number in a random way within these limits (Fig. 3). The most intense of them are also smaller than f_1 and f_2 by 0.1–0.5 GHz. This result can be explained on the basis that the SBS-90 occurs not only along the axis of the capillary but also at scattering angles close to $\vartheta = 90^\circ$, predominantly at $\vartheta < 90^\circ$. The SBS emission undergoes several reflections from the walls of the capillary before it leaves the capillary. For smaller values of ϑ , the absorption coefficient for the hypersonic wave decreases, and the SBS-90 intensity rises.

In the spectra in Figs. 2 and 3 we see a frequency $f_3 \sim 1.8$ –2 GHz, and in $C(\tau)$ we see maxima (Fig. 3) or an inflection point (Fig. 2) in the corresponding time interval, 0.55–0.65 ns. An interpretation of this frequency as the subharmonic $(1/3)f_1$ or $(1/4)f_2$ is extremely dubious, since at the very beginning of the development of the SBS-90 we sometimes observe low-intensity oscillations with a period of 0.45–0.7 ns (Sec. V), which could not be seen visually against the background of the large-scale oscillations.

In $C(\tau)$ (Figs. 2b and 3), we see a maximum at 0.73–0.77 ns ($f_4 \sim 1.3$ –1.4 GHz). This frequency is not present in the spectra in Figs. 2 and 3, but frequencies in the interval $f_4 \sim 1.4$ –1.6 GHz are seen in an expanded analysis of low frequencies of the spectra. At this point, the interpretation of f_3 and f_4 is unclear.

8. The large-scale intensity oscillations of the SBS which are observed (≈ 2 –6 ns) are similar to the relaxation oscillations in the SBS-180, because of a depletion of the pump intensity by the counterpropagating stimulated scattering,⁵ the period of which, $2T_0$, is increased because of the long phonon lifetime.³ This depletion mechanism does not operate in the case of transverse pumping. However, when the SBS-90 arises in one direction, for this emission to be amplified again and to leave in the same direction, it must pass through the medium at least twice or, depending on the ratio between the gain and loss coefficients, $2m$ times (where m is an integer), intensifying by a factor of m in the process. It is apparently for this reason that the time intervals of $2mT_0$ between peaks arise.

If the SBS-90 develops simultaneously in two opposite directions, the temporal structure becomes more complex. A temporal instability can develop in the counterpropa-

gating SBS-90 beams (see Ref. 6 and the papers cited there), leading to a modulation of the intensity at the frequency of the SBS¹ and its subharmonics, as observed in our own experiments. Strong stricitive and orientational⁴ nonlinearities, promoting the onset of subharmonics and harmonics and their mixing, may ultimately lead to the onset of dynamic chaotic structures.

We wish to thank I. K. Fabelinskiĭ for interest in this study and for a discussion of the results. We also thank V. V. Oleĭnikov for assistance.

This study had financial support from the Russian Fund for Fundamental Research (Project 930214279).

¹A. L. Gaeta *et al.*, J. Opt. Soc. Am. B **6**, 1709 (1989).

²O. Kulagin *et al.*, J. Opt. Soc. Am. B **8**, 2155 (1991).

³E. M. Dianov *et al.*, Opt. Quantum Electron. **21**, 381 (1989).

⁴W. Lu, A. Johnstone and R. G. Harrison, Phys. Rev. A **46**, 4114 (1992).

⁵R. V. Johnson and J. H. Marburger, Phys. Rev. A **4**, 1175 (1971).

⁶B. Ya. Zel'dovich *et al.*, *Principles of Phase Conjugation* (Springer-Verlag, New York, 1985).

Translated by D. Parsons